Hetero-bimetallic paddlewheel clusters in coordination polymers formed by a water-induced single-crystal-to-single-crystal transformation

Jorge Albalad, Javier Aríñez-Soriano, José Vidal-Gancedo, Vega Lloveras, Inhar Imaz, Núria Aliaga-Alcalde and Daniel Maspoch

Herein we report a water-induced single-crystal to single-crystal transformation that involves the formation of hetero-bimetallic paddlewheel clusters in coordination polymers. Through this transformation, which involves the cleavage and formation of different coordination bonds, two different Cu(II)-Zn(II) and Cu(II)-Ni(II) paddlewheel units exhibiting a 1:1 metal ratio were created.

Coordination polymers (CPs), including porous metal-organic frameworks (MOFs), exhibit a very rich organic-inorganic chemistry that makes possible their structural and compositional design for myriad applications.[1–5] This design is mostly succeeded through the careful choice of the building blocks (that is, the organic linker and the metal ion),[6–8] or by inducing post-synthetic transformations onto metastable phases.[9–12] To date, most of these post-synthetic transformations are made on the organic linkers. However, an increasing interest is recently focused on exchanging metal ions in the inorganic units using post-synthetic metalation (PSM) pathways.[13,14] This latter strategy allows the creation of more "exotic" heterometallic inorganic units in CPs that can optimize, for example, their stability,[15,16] gas sorption,[17,18] catalytic activity[19], luminescence[20] and magnetic properties.[21]

Among all potential clusters present in the literature of CPs/ MOFs,[22] the organometallic paddlewheel unit is probably one of the best candidate for the study of the above-mentioned metalation processes due to its centrosymmetric character and structural simplicity. This cluster is relatively easy to synthesize using a wide range of metal sources, including Cu, Ni, Zn, Co, Mn, Cd, Ru, or even Bi-Rh,[23] among others. Based on it, some advances have already been made on creating hetero-bimetallic paddlewheel clusters using PSM.[24–26] For example, Zn(II)-Cu(II) units were introduced in HKUST-1 by starting with a pure Zn(II)-HKUST-1 sample and making PSM with $Cu(NO_3)\cdot2.5H_2O$.[27] Also, bimetallic Zn(II)-M(II) (where M is Cu, Ni and Co) paddlewheel units in two CPs were produced starting from pure Zn(II)-paddlewheel units.[28] However, the governing factors of PSM are still uncertain and a successful insertion of a specific metal ion is usually achieved using empirical trial-and-error methodologies, provoking also uncontrolled substitutions in which is unclear the exact spatial disposition adopted by the new ions.[29]

Another approach for designing novel heterometallic clusters (and in particular, hetero-bimetallic paddlewheel clusters) in a more controlled way should be their formation during the CP synthesis. Using this approach, Kleist *et al.* synthesized HKUST-1 made of paddlewheel units containing Cu(II) and Ru(II).[25] However, the content of Ru(II) in this HKUST-1 was very low, meaning that only 9 % of the units should potentially be hetero-bimetallic units. To our knowledge, there is only one example of pure hetero-bimetallic paddlewheel units with a 1:1 metal ratio done using this strategy.[30] Doonan *et al.* successfully showed the formation of discrete polyhedra made of Pd(II)-M(II) (where M is Zn, Cu and Ni) paddlewheel units starting from preformed bimetallic acetates as reagents.[31]

Herein we show the formation of two hetero-bimetallic Cu(II)-Zn(II) and Cu(II)-Ni(II) paddlewheel clusters exhibiting a 1:1 metal ratio in two isostructural CPs (hereafter called **2$_{CuZn}$** and **2$_{CuNi}$**). These CPs are made from water-induced single-crystal to single-crystal (SC-SC) transformations of preformed hetero-bimetallic CPs (hereafter called **1$_{CuZn}$** and **1$_{CuNi}$**) that do not contain the paddlewheel units.

1$_{CuZn}$ was initially obtained through a two-step synthesis.[32] In a first step, the macrocyclic Cu-DOTA complex was precipitated by mixing $CuCl_2\cdot2H_2O$ (0.075 mmol) and 1,4,7,10-tetraazacyclododecane-1,4,7,10-tetraacetic acid (H$_4$DOTA; 0.075 mmol) in water (4 mL) under sonication for 5 min at room temperature (Fig. S1, ESI†). In a second step, a DMF solution (4 mL) containing $Zn(NO_3)\cdot6H_2O$ (0.15 mmol) was added into the aqueous solution containing the synthesized Cu-DOTA complex under stirring. This mixture was then transferred to high temperature capped vials and allowed to react at 120 ºC, from which plate-shaped sky blue crystals suitable for single-crystal X-Ray diffraction (SCXRD) were collected after 12 hours (yield: 66 %; obtained as a pure phase, as confirmed by elemental analysis, energy-dispersive X-ray spectroscopy (EDX), inductively coupled plasma optical emission spectrometry (ICP-OES) and X-ray powder diffraction (XRPD); Tables S2,S3 and Fig. S2, ESI†). **1$_{CuZn}$** crystallized in the monoclinic P2/n symmetry group with formula [ZnCu(DOTA)(H$_2$O)] (Table S1, ESI†). A closer analysis on **1$_{CuZn}$** revealed the formation of a 2D framework extended along the *ac* plane. In these layers, Cu(II) ions are accommodated inside the macrocyclic cavity adopting a distorted octahedral geometry coordinated to the cyclen subunit and to two of the acetate arms (Fig. 1a). These two arms act as bidentate bridges (η_2) between the Cu(II) and Zn(II) ions. Zn(II) extends the framework in a square-based pyramid motif (Fig. 1b) using not only the two η_2 bridge carboxylate arms along the *a* axis but also the open η_1 arms along the perpendicular *c* axis. The coordination environment around Zn(II) is completed with the presence of a water molecule (O$_1$W) crowning the axial position of the pyramid. The different layers are packed in an AAA sequence connected via hydrogen bonds between O$_1$W and the non-coordinated oxygen atoms in the η_1 carboxylate arms of a subsequent layer (Fig. S3, ESI†). Remarkably, the resulting framework is compact, meaning that there are not guest solvent molecules in the structure.

Because of Cu(II) and Zn(II) are undistinguishable through SCXRD, the location of Cu(II) ions in 1_{CuZn} was further investigated by electronic paramagnetic resonance (EPR). To study the former, we performed measurements on 1_{CuZn} and compared with that of the discrete macrocyclic complex Cu-DOTA.[33] As expected, Cu-DOTA showed the characteristic EPR spectrum of a Cu(II) complex with an elongated octahedral geometry (Fig. 2a). The $g_{\parallel}$ and $g_{\perp}$ values were 2.260 and 2.097, respectively. Importantly, the EPR spectrum of 1_{CuZn} was very similar to that of Cu-DOTA, with $g_{\parallel}$ and $g_{\perp}$ values of 2.210 and 2.104, respectively. This similarity confirmed that indeed the Cu(II) ions reside inside the macrocyclic cavities in 1_{CuZn}, and that the Zn(II) ions bridge these Cu-DOTA units. It is important to highlight here that this evidence is also in good agreement with the reported Cu/Zn association constants with H_4DOTA (Log K_d= 22.72 and 18.70 for Cu-DOTA and Zn-DOTA, respectively).[34] Finally, to discard the presence of Cu(II) ions in the metal positions responsible of bridging the macrocyclic complexes, we finally compared our previous spectra with that obtained for the isostructural homometallic 1_{CuCu}. Note here that 1_{CuCu} was prepared using the same conditions as for 1_{CuZn}, except that instead of $Zn(NO_3)\cdot6H_2O$ in the second synthetic step, we used $Cu(NO_3)_2\cdot2H_2O$ (yield: 87 %; obtained as a pure phase, as confirmed by elemental analysis and XRPD; Fig. S2, ESI†). In this case, the EPR spectrum was quite different, exhibiting $g_{\parallel}$ and $g_{\perp}$ values of 2.140 and 2.128, respectively (Fig. 2a). Since Cu(II) ions in 1_{CuCu} adopt not only an elongated octahedral geometry but also a square pyramidal geometry, these results confirmed the absence of Cu(II) ions outside the macrocycle in 1_{CuZn}.

Crystals of 1_{CuZn} (and also of 1_{CuCu}) were thermodynamically unstable in their reaction medium, undergoing a spontaneous SC-SC transition when left undisturbed for weeks. Moreover, this SC-SC transformation could be accelerated when dry crystals of 1_{CuZn} were soaked in pure distilled water without any addition of external metal sources for 72 hours (96 hours for 1_{CuCu}; Fig. S4,S5, ESI†). Remarkably, the resulting prism-shaped green crystals of 2_{CuZn} were suitable for SCXRD. 2_{CuZn} crystallized in the P21/c symmetry group showing a theoretical formula of $[Zn_xCu_{2-x}(DOTA)(H_2O)]\cdot4H_2O$ (the crystal structure was solved considering x = 1; Table S1, ESI†). 2_{CuZn} shows a 2D framework in which the Cu(II) ions also reside in the macrocyclic cavity adopting the same distorted octahedral geometry. However, unlike in 1_{CuZn}, the closed pendant arms do not contribute to extend the coordination layers. Instead, the coordination layers in 2_{CuZn} are expanded along the *ab* plane through the open arms forming $M_2(COO)_4$ paddlewheel clusters (Fig. 1b). The different layers are then stacked in an ABAB sequence forming 1D channels along the *c* axis, which are filled with guest water molecules (Fig. S6, ESI†). Interestingly, 2_{CuZn} was stable in water for at least 6 months (Fig. S7, ESI†), and their guest water molecules could be removed and re-adsorbed without affecting the integrity of the open-framework (Fig. S8, S9, ESI†). Indeed, water adsorption measurements showed a standard Type I isotherm with a water uptake of 0.12 $g_{water}\cdot g_{2CuZn}^{-1}$ at 30 % RH, which corresponds to 4.2 water molecules. The isotherm shows then a plateau from 25% to 65 % RH and, after that, 2_{CuZn} gained hydrophilicity adsorbing up to 0.21 $g_{water}\cdot g_{2CuZn}^{-1}$.
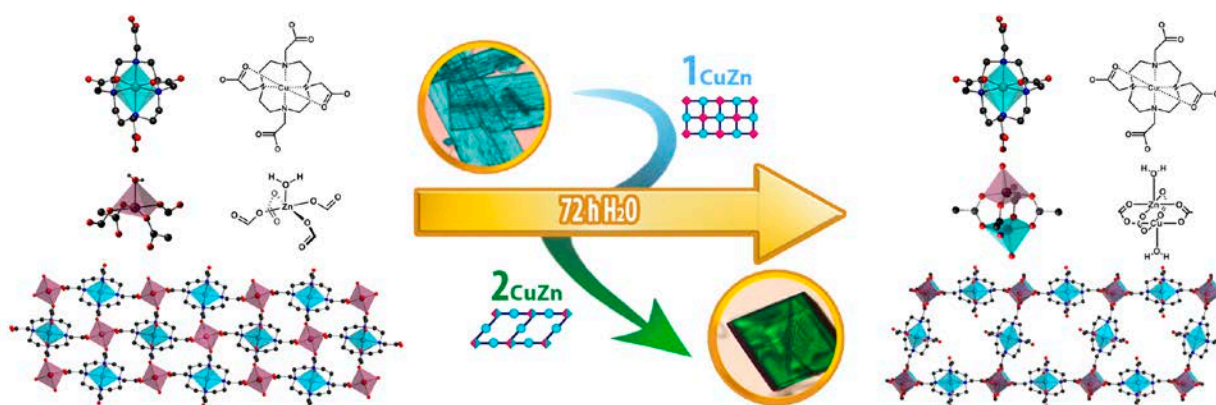

Fig. 1. Schematic representation of the water-triggered transition from 1_{CuZn} to 2_{CuZn}. For both sides: (top) Representation of the Cu-DOTA illustrating the octahedral coordination geometry (blue octahedron); (middle) Representation of the square-based pyramidal coordination geometry of Zn(II) ions in 1_{CuZn} (purple tetrahedron), which is transformed to an hetero-bimetallic Cu(II)-Zn(II) paddlewheel unit in 2_{CuZn} (purple tetrahedron for Zn(II) and blue tetrahedron for Cu(II)); and (bottom) 2-D frameworks of 1_{CuZn} (left) and 2_{CuZn} (right).

To obtain more details of the composition of $\mathbf{2_{CuZn}}$, we then analyzed it using EDX and ICP-OES (Table S4,S5, ESI†). Surprisingly, the multiple measurements done with both techniques never suggested an equal proportion (x = 1) of Cu(II) and Zn(II) ions but always a precise 3:1 Cu(II) : Zn(II) ratio (or x = 0.5). These results lead to a final formula for $\mathbf{2_{CuZn}}$ of $[Zn_{0.5}Cu_{1.5}(DOTA)(H_2O)]\cdot 4H_2O$. Thus, considering that the metal position inside the macrocycle is occupied by Cu(II), the two metal positions of the paddlewheel units must be occupied by a 1 : 1 mixture of Cu(II) and Zn(II) ions.

To further confirm the formation of the bimetallic 1:1 Zn(II):Cu(II) paddlewheel units, we performed magnetic susceptibility measurements on both $\mathbf{2_{CuZn}}$ and $\mathbf{2_{CuCu}}$ (Fig. 2b). If the hetero-bimetallic Cu(II)-Zn(II) units are formed, the paramagnetic Cu(II) ions located inside the macrocycles and those forming the paddlewheel units are quite separated, so that only weak intermolecular magnetic interactions at very low temperatures are expected. On the contrary, strong antiferromagnetic interactions at high temperatures are already expected if homometallic Cu(II)-Cu(II) paddlewheel units are present in $\mathbf{2_{CuZn}}$. Indeed, homometallic Cu(II)-Cu(II) paddlewheel units display a rather strong antiferromagnetic behavior, providing exchange coupling constants of J values

Fig. 3 Schematic representation of the mechanism. Note that Cu(II)[*] represents the insertion of Cu(II) coming from the release of Cu-DOTA due to the degradation of the crystal.

between -200 cm^{-1} and -1000 cm^{-1}.[35] With this in mind, solid-state variable-temperature (1.8 K - 300.0 K) dc magnetic susceptibility data of polycrystalline samples of $\mathbf{2_{CuZn}}$ and $\mathbf{2_{CuCu}}$ using a 1.0 T field were collected. Their magnetic behaviors are depicted in Fig. 2 as plots of X_MT vs T. In both cases, TIP corrections were performed by adding $-60\cdot10^{-6}$ cm^3 mol^{-1} K per Cu(II) unit. The X_MT values at 300 K were 0.72 cm^3 mol^{-1} K for $\mathbf{2_{CuCu}}$ and 0.56 cm^3 mol^{-1} K for $\mathbf{2_{CuZn}}$, which are in good agreement with those expected for one and a half independent Cu(II) centers in $\mathbf{2_{CuCu}}$ (0.74 cm^3 mol^{-1} K) and for one Cu(II) center in $\mathbf{2_{CuZn}}$ (0.55 cm^3 mol^{-1} K); considering a g value of 2.00 in both cases. As expected, the X_MT values of $\mathbf{2_{CuCu}}$ rapidly decreased upon cooling, consistent with the presence of strong antiferromagnetic coupling between the two Cu(II) ions forming the homometallic paddlewheel units. In quite contrast, the X_MT values for $\mathbf{2_{CuZn}}$ remained almost constant all over the temperatures, and slightly decreased below 25 K. This behavior is characteristic of a system that is weakly coupled, as expected for a $\mathbf{2_{CuZn}}$ system built up from hetero-bimetallic Cu(II)-Zn(II) paddlewheel units.
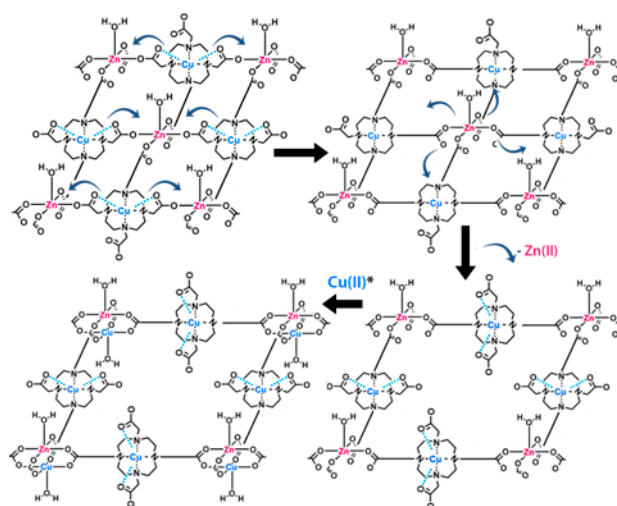
Fig. 3 shows an hypothetic mechanism proposed for the formation of these hetero-bimetallic paddlewheel units, which starts with a dynamic cleavage of the η_2 acetate arms on **1$_{CuZn}$** through the Cu-O bond, induced by the presence of water (first fragment of Fig. 3). This step triggers the formation of a metaphase where all the pendant arms are equally open (second fragment of Fig. 3). This metaphase can therefore be seen as "half-empty" paddlewheel units. The transition continues when half of these open arms rearrange to complete again the thermodynamically favorable octahedral coordination around the Cu(II) ions, leaching to the solution half of the Zn(II) ions (third fragment of Fig. 3). A partial dissociation of the material should happen afterwards in order to compensate the charge unbalance, releasing and equal value of [Cu-DOTA]$^{2-}$ units to the solution. Half of these released Cu(II) ions must be able to complete the holes on the half-formed paddlewheel units, finally forming the hetero-bimetallic clusters found in **2$_{CuZn}$** (forth fragment of Fig. 3). This hypothetic mechanism implies the loss of 41 % of the initial weight of the crystals as well as the release of 50 % and 25 % of the initial Zn(II) and Cu(II) ions, respectively. To follow these parameters, we immersed crystals of **1$_{CuZn}$** (17.8 mg) in water (5.0 ml) and followed their SC-SC transformation to **2$_{CuZn}$**. After 72 hours, the transition was completed, and 9.8 mg of **2$_{CuZn}$** were collected, corresponding to a weight loss of 45 %. In addition, the water solution was analyzed by ICP-OES, and found a Zn(II) and Cu(II) content of 0.49 mg (98 ppm) and 1.03 mg (206 ppm), respectively. These amounts correspond to a weight loss of 26 % and 51 % of the initial Zn(II) and Cu(II) content in **1$_{CuZn}$**. Altogether, these results evidence the feasibility of our proposed mechanism.

Finally, to expand the variety of hetero-bimetallic paddlewheel units, we reproduced the synthesis of **1$_{CuZn}$** but using nitrate salts of Mn(II), Fe(II)/(III), Co(II), Ni(II), Ag(I) or Pd(II) in the second step. Among these different metal ions, we could only confirm the formation of **1$_{CuNi}$** (yield: 71 %; obtained as a pure phase, as confirmed by XRPD, EDX, ICP-OES and elemental analysis; Tables S2,S3 and Fig. S2, ESI†). Remarkably, we found that the transition **1$_{CuNi}$** →**2$_{CuNi}$** was also possible after immersing **1$_{CuNi}$** in water for two months. Here, EDX and ICP-OES analysis also gave a 3:1 Cu(II) : Ni(II) ratio (Table S4, S5, ESI†), thus confirming the formation of the hetero-bimetallic Cu(II)-Ni(II) paddlewheel units in **2$_{CuNi}$**.

In conclusion, we have shown the unprecedented formation of isostructural CPs that contain hetero-bimetallic paddlewheel units having a 1:1 metal ratio inside the cluster. This formation takes place by a water-induced SC-SC transformation from a compact hetero-bimetallic framework built up from connecting Cu-DOTA units through isolated metal ions to a more open framework built up from connecting identical Cu-DOTA units through hetero-bimetallic paddlewheel units. This SC-SC transformation was reproduced for two different cases allowing the formation of two Cu(II)-Zn(II) and Cu(II)-Ni(II) paddlewheel units. This study illustrates the diversity, richness and beauty of this type of chemistry, from which many new systems remain to be discovered.
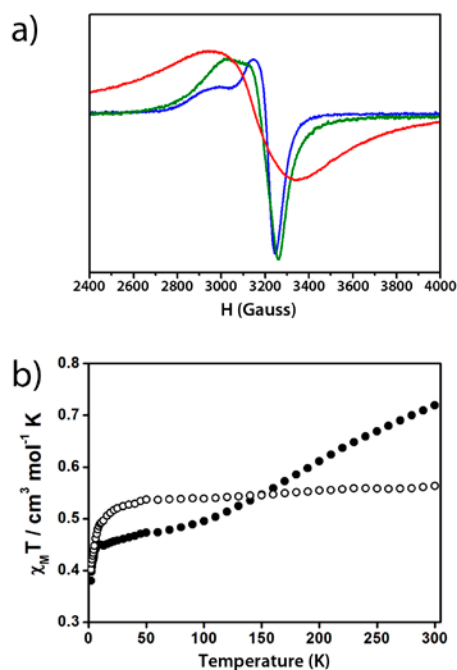

Fig. 2. (a) EPR Spectra for CuDOTA (blue), **1$_{CuZn}$** (green) and **1$_{CuCu}$** (red). An octahedral environment around Cu(II) ions can be attributed to the initial heterometallic phase. (b) Experimental $\chi_M T$ vs T data of systems **2$_{CuCu}$** (●) and **2$_{CuZn}$** (○) between 2.0 K and 300.0 K using a dc external magnetic field of 1T.

Notes and references

1   C. Janiak, *Dalt. Trans.*, 2003, 2781.
2   S. Kitagawa, R. Kitaura and S. Noro, *Angew. Chemie Int. Ed.*, 2004, **43**, 2334–75.
3   K. M. Fromm, *Angew. Chemie Int. Ed.*, 2009, **48**, 4890–4891.
4   D. Zhao, D. J. Timmons, D. Yuan and H. C. Zhou, *Acc. Chem. Res.*, 2011, **44**, 123–133.
5   B.-L. Liu, H.-Y. Zang, H.-Q. Tan, Y.-H. Wang and Y.-G. Li, *CrystEngComm*, 2016, **18**, 3300–3305.
6   X. Zhang, Z. Zhang, J. Boissonnault and S. M. Cohen, *Chem. Commun.*, 2016, **52**, 8585–8588.
7   F. A. Almeida Paz, J. Klinowski, S. M. F. Vilela, J. P. C. Tomé, J. A. S. Cavaleiro and J. Rocha, *Chem. Soc. Rev.*, 2012, **41**, 1088–1110.
8   A. J. Fletcher, K. M. Thomas and M. J. Rosseinsky, *J. Solid State Chem.*, 2005, **178**, 2491–2510.
9   A. Béziau, S. A. Baudron, G. Rogez and M. W. Hosseini, *Inorg. Chem.*, 2015, **54**, 2032–2039.
10 S. Yang, L. Liu, J. Sun, K. M. Thomas, A. J. Davies, M. W. George, A. J. Blake, A. H. Hill, A. N. Fitch, C. C. Tang and M. Schr??der, *J. Am. Chem. Soc.*, 2013, **135**, 4954–4957.
11 M. H. Mir, L. L. Koh, G. K. Tan and J. J. Vittal, *Angew. Chemie Int. Ed.*, 2010, **49**, 390–393.
12 M. R. Warren, S. K. Brayshaw, A. L. Johnson, S. Schiffers, P. R. Raithby, T. L. Easun, M. W. George, J. E. Warren and S. J. Teat, *Angew. Chemie Int. Ed.*, 2009, **48**, 5711–5714.
13 C. K. Brozek and M. Dincă, *Chem. Soc. Rev.*, 2014, **43**, 5456–5467.
14 J. D. Evans, C. J. Sumby and C. J. Doonan, *Chem. Soc. Rev.*, 2014, **43**, 5933–5951.
15 A. Bajpai, P. Chandrasekhar, S. Govardhan, R. Banerjee and J. N. Moorthy, *Chem. - A Eur. J.*, 2015, **21**, 2759–2765.
16 T. Grancha, J. Ferrando-Soria, H. C. Zhou, J. Gascon, B. Seoane, J. Pasán, O. Fabelo, M. Julve and E. Pardo, *Angew. Chemie Int. Ed.*, 2015, **54**, 6521–6525.
17 S. Yang, X. Lin, A. J. Blake, G. S. Walker, P. Hubberstey, N. R. Champness and M. Schröder, *Nat. Chem.*, 2009, **1**, 487–493.
18 S. Yang, G. S. B. Martin, J. J. Titman, A. J. Blake, D. R. Allan, N. R. Champness and M. Schröder, *Inorg. Chem.*, 2011, **50**, 9374–9384.
19 L. Ma, J. M. Falkowski, C. Abney and W. Lin, *Nat. Chem.*, 2010, **2**, 838–846.
20 P. R. Matthes, C. J. Hoeller, M. Mai, J. Heck, S. J. Sedlmaier, S. Schmiechen, C. Feldmann, W. Schnick and K. Mueller-Buschbaum, *J. Mater. Chem.*, 2012, **22**, 10179–10187.
21 C. K. Brozek, V. K. Michaelis, T.-C. Ong, L. Bellarosa, N. López, R. G. Griffin and M. Dincă, *ACS Cent. Sci.*, 2015, **1**, 252–260.
22 D. J. Tranchemontagne, J. L. Mendoza-Cortés, M. O'Keeffe and O. M. Yaghi, *Chem. Soc. Rev.*, 2009, **38**, 1257.
23 T. L. Sunderland and J. F. Berry, *Dalt. Trans.*, 2016, **45**, 50–55.
24 T. K. Pal, S. Neogi and P. K. Bharadwaj, *Chem. - A Eur. J.*, 2015, **21**, 16083–16090.
25 M. A. Gotthardt, R. Schoch, S. Wolf, M. Bauer and W. Kleist, *Dalt. Trans.*, 2015, **44**, 2052–6.
26 R. Zou, P. Z. Li, Y. F. Zeng, J. Liu, R. Zhao, H. Duan, Z. Luo, J. G. Wang, R. Zou and Y. Zhao, *Small*, 2016, **12**, 2334–2343.
27 X. Song, S. Jeong, D. Kim and M. S. Lah, *CrystEngComm*, 2012, **14**, 5753.
28 T. K. Pal, S. Neogi and P. K. Bharadwaj, *Chem. - A Eur. J.*, 2015, **21**, 16083–16090.
29 F. Gul-E-Noor, B. Jee, M. Mendt, D. Himsl, A. Pppl, M. Hartmann, J. Haase, H. Krautscheid and M. Bertmer, *J. Phys. Chem. C*, 2012, **116**, 20866–20873.
30 J. M. Teo, C. J. Coghlan, J. D. Evans, E. Tsivion, M. Head-Gordon, C. J. Sumby and C. J. Doonan, *Chem. Commun.*, 2015, **52**, 276–279.
31 N. Y. Kozitsyna, S. E. Nefedov, F. M. Dolgushin, N. V. Cherkashina, M. N. Vargaftik and I. I. Moiseev, *Inorg. Chim. Acta*, 2006, **359**, 2072–2086.
32 J. Aríñez-Soriano, J. Albalad, J. Pérez-Carvajal, I. Imaz, F. Busqué, J. Juanhuix and D. Maspoch, *CrystEngComm*, 2016, **37**, 191–214.
33 A. Riesen, M. Zehnder and T. a Kaden, *Helv. Chim. Acta*, 1986, **69**, 2067–2073.
34 N. Viola-Villegas and R. P. Doyle, *Coord. Chem. Rev.*, 2009, **253**, 1906–1925.
35 M. Fontanet, A. R. Popescu, X. Fontrodona, M. Rodríguez, I. Romero, F. Teixidor, C. Viñas, N. Aliaga-Alcalde and E. Ruiz, *Chem. - A Eur. J.*, 2011, **17**, 13217–13229.